

# Study of In Vitro Biodegradation Behavior of Mg–2.5Zn–xES Composite

Srinivasan Murugan, Paul C. Okonkwo, Ahmed Bahgat, Gururaj Parande, Aboubakr M. Abdullah, and Manoj Gupta

## Abstract

In this study, zinc (Zn) and eggshell (ES) reinforced biodegradable magnesium alloy (Mg–2.5Zn) and environment concise (eco) composite (Mg–2.5Zn–xES) was fabricated using disintegrated melt deposition (DMD) technique. In vitro experiments were conducted to study the biodegradation behavior of Mg–2.5Zn and Mg–2.5Zn–xES ( $x = 3$  and  $7$  wt%) using simulated body fluid (SBF) under standard human body temperature of  $37$  °C. Using electrochemical Impedance Spectroscopy (EIS), electrochemical analysis was performed to study in vitro degradation behavior of alloy and composite. EIS revealed increased in vitro degradation of the biodegradable magnesium alloy and ecofriendly composite as percentage of ES reinforcement was increased. X-ray diffraction (XRD) was performed to observe the chemical composition of elements and reaction products present in the degraded samples after corrosion process. Scanning electron microscopy (SEM) analysis showed variations in surface morphology of the alloy and composite before and after degradation. SEM result revealed presence of defects in the tested samples after degradation process.

## Keywords

Magnesium • Eggshell • DMD • Biodegradation • SBF • EIS

## Introduction

Increasing demand to reduce greenhouse gas emissions has made the researchers to explore and develop lightweight materials at economical price, since the beginning of twenty-first century [1]. For the past two decades, magnesium (Mg) has emerged as a potential candidate in decreasing use of steel and aluminium. Mg has found its application in aerospace, automotive, sporting, and biomedical equipment due to less density and higher specific strength [1–4]. Stainless steel (SS) and titanium (Ti) are used as permanent/temporary human body implant for more than a century in biomedical application [4]. SS/Ti with higher elastic modulus used as orthopedic implants has major drawback of high stress shielding. Bioresorbable Mg has relatively closer elastic modulus compared to that of the natural bone which reduces the stress shielding effect as well as reduces healing time [5, 6]. Bioresorbable characteristics of Mg cause it to dissolve in human body which eliminates the cost of revision surgery and patients risk from surgical procedures. Mg is an essential mineral for metabolism in human body and the excess drained out in the form of urine [7].

Degradation/corrosion rate of pure Mg limits its use as orthopedic implant to maintain structural strength in physiological environment. Alloying elements for biomedical application are determined based on availability and ease of disposal, toxicity, and biocompatibility. Proper choice of alloying elements like Calcium (Ca), Zinc (Zn), Tin (Sn), Zirconium (Zr), etc., can control the rate of corrosion over stipulated period [8]. Zn is abundant in nature with high nutritional value, able to improve the corrosion resistant and highly biodegradable in physiological environment [9]. While Ca stimulates human bone growth, addition of Ca to Mg improves the mechanical properties and corrosion resistance of the material implanted in the human body [9]. Researches were performed to add eggshell that contains 95% of calcium carbonate and the hydroxyapatite derived

S. Murugan (✉) · P. C. Okonkwo  
Department of Mechanical and Mechatronics Engineering,  
Dhofar University, Salalah, Oman  
e-mail: [smurugan@du.edu.om](mailto:smurugan@du.edu.om)

A. Bahgat · A. M. Abdullah  
Centre for Advanced Materials, Qatar University, Doha, Qatar

G. Parande · M. Gupta  
Department of Mechanical Engineering, National University of  
Singapore, Singapore, Singapore

from eggshell synthesis used as bone graft material [10–12]. Ca is a natural source in eggshell waste which used as a reinforcement in Mg matrix to form eco (environmental concise) composite [13]. The results showed a considerable increase in mechanical properties and damping behavior at room temperature [14]. Damping is considered to be an important parameter which aids in mitigating the vibrations prolonged into human body caused by movements of the recipient and the stresses induced in the bone-implant interface.

This study focused on understanding the in vitro corrosion behavior of pure Mg alloyed with Zn and reinforced with xES ( $x = 0, 3, 7\%$ ) in a SBF at 37 °C. The prepared biodegradable composite was subjected to EIS analysis for two weeks. The materials were initially prepared using disintegrated melt deposition (DMD) [15–17] and hot extruded to 8 mm diameter. Then, the samples were further polarized to study the biodegradation behavior using EIS. SEM and XRD were employed to characterize the surface morphology and chemical composition of the Mg–2.5Zn–xES composite.

## Materials and Methods

The biodegradable magnesium alloys were prepared by melting pure Mg under argon gas jacket along with 2.5 wt% Zn and varying amount of eggshell ( $x = 3 \text{ wt\%}$  and  $7 \text{ wt\%}$  designated as 3ES and 7ES, respectively) to form three different material composition. Pure Mg turnings, powders of Zn and eggshell stacked like sandwich in a graphite crucible, was then superheated to a temperature of 750 °C and stirred with zirtex 25 [18] coated steel stirrer. The stirring was carried to form a vortex for 5 min at 450 rev/min. The melt was tapped at the bottom of the crucible through a graphite nozzle at 25 Lpm. The disintegrated melt was deposited into a graphite coated steel substrate to form cast billets of 50 mm in diameter. Furthermore, hot extrusion was carried to homogenize the cast billet using 150 T hydraulic press. The hot extrusion was carried at 350 °C to obtain the

billets of 8 mm in diameter with an extrusion ratio of 20.25:1. Colloidal graphite was used as lubricant.

A three-electrode double-jacketed 250 ml in vitro corrosion cell was used, in which a graphite rod, Mg coupon (only 50 mm<sup>2</sup> is exposed to the SBF), and saturated calomel electrode were the counter, working and reference electrodes, respectively [19]. The cell was maintained at 37 °C  $\pm$  0.5 °C using a thermostat water circulator. A thermometer was used to monitor the temperature of the electrolyte before and during the experiments. A Reference GAMRY 3000 potentiostat (Warminster, PA, USA) was used to perform the electrochemical measurements. Electrochemical impedance spectroscopy (EIS) measurements of Mg alloys were investigated for 2 weeks immersion in SBF solution in a frequency range of 10<sup>-2</sup> to 10<sup>5</sup> Hz with an AC amplitude of 5 mV. Tafel experiment was carried out at a constant scan rate of 0.3 mV/s within scan range of  $\pm$ 250 mV versus the open-circuit potential (OCP). The SBF composition was prepared as described in Table 1 [20].

Characterizing the degraded surfaces is vital to analyze the in vitro corrosion behavior of the samples after EIS electrochemical analysis. XRD (X'Pert-Pro MPD, PANalytical Co., Netherlands) was utilized to study different phases on the in vitro corroded samples. The morphology of the corroded surface was examined by Field emission scanning electron microscopy (FEI NOVA NANOSEM 450, Hillsboro, OR, USA) with an accelerating voltage of 20 kV.

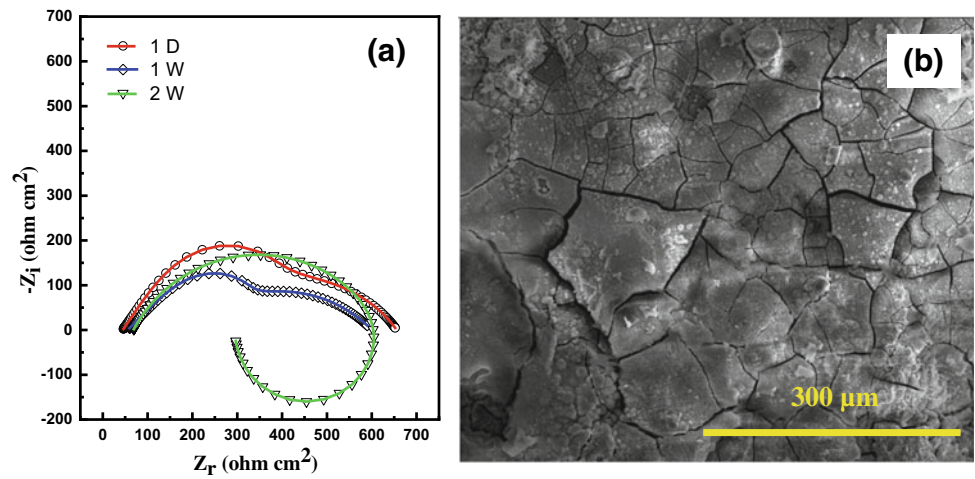
## Results and Discussion

The in vitro degradation of Mg–2.5Zn alloy and eco-composites using electrochemical impedance spectroscopy (EIS) was carried in simulated physiological environment. As shown in Figs. 1a, 2a and 3a, Nyquist plots revealed the in vitro degradation behaviors of the bioresorbable Mg samples. Nyquist plots showed the data obtained for 2 W (336 h) of immersion. The trend in the loops shows the corrosion rate evolution of the tested samples at different immersion duration.

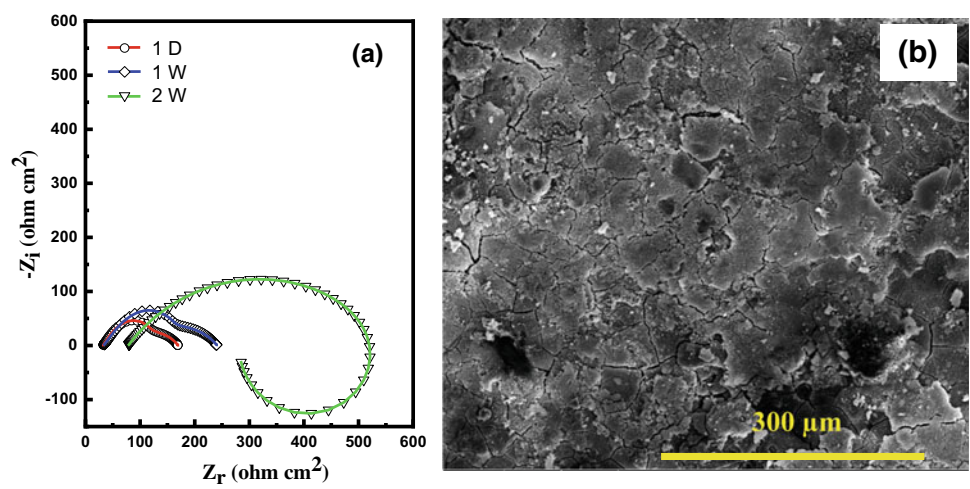
**Table 1** Regents for preparing SBF (pH7.40, 1 L) [20]

Order	Reagent	Amount
1	NaCl	8.035 g
2	NaHCO <sub>3</sub>	0.355 g
3	KCl	0.225 g
4	K <sub>2</sub> HPO <sub>4</sub> · 3H <sub>2</sub> O	0.231 g
5	MgCl <sub>2</sub> · 6H <sub>2</sub> O	0.311 g
6	1 M HCl	39 mL
7	CaCl <sub>2</sub>	0.292 g
8	Na <sub>2</sub> SO <sub>4</sub>	0.072 g
9	(CH <sub>2</sub> OH) <sub>3</sub> CNH <sub>2</sub>	6.118 g
10	1.0 M HCl	0–5 mL

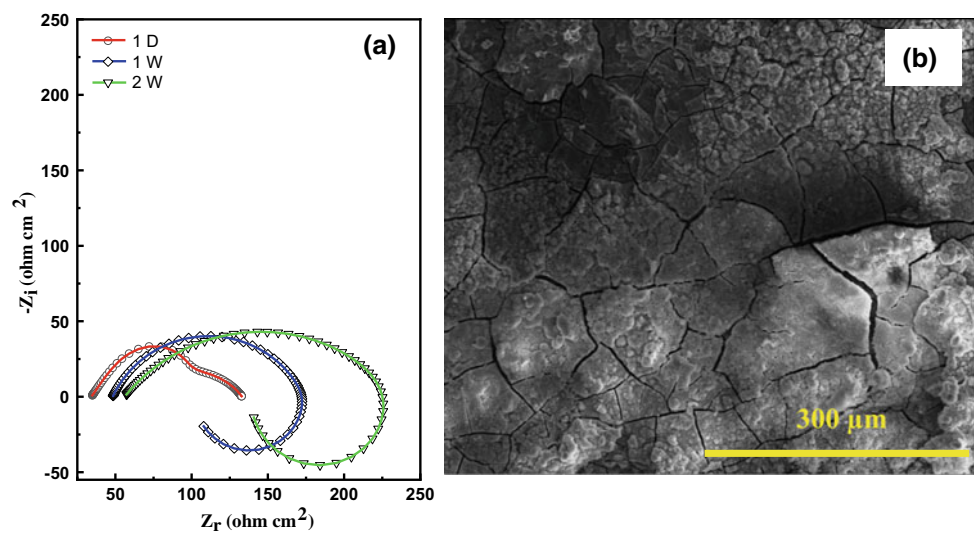
**Fig. 1** Mg-2.5Zn **a** Nyquist plot, **b** SEM image of degraded surface after 336 h (2 W)



**Fig. 2** Mg-2.5Zn-3ES **a** Nyquist plot, **b** SEM image of degraded surface after 336 h (2 W)



**Fig. 3** Mg-2.5Zn-7ES **(a)** Nyquist plot **(b)** SEM image of degraded surface after 336 h (2 W)



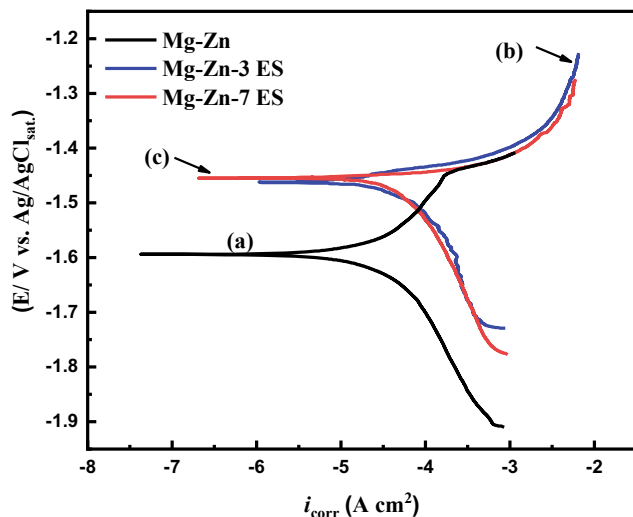
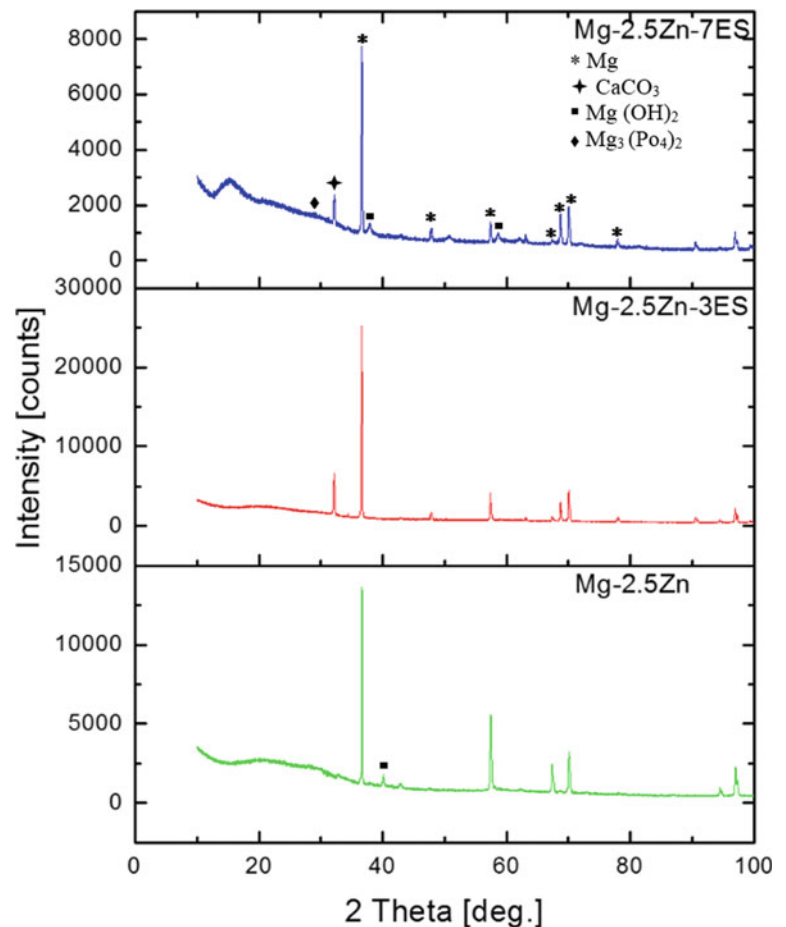


**Fig. 4** Tafel curves of a Mg-Zn, Mg-Zn-3ES and Mg-Zn-7ES alloys specimens in SBF solution

From the plots, it is evident that the curves are categorized by a semicircle in the high and middle region and a capacitive semicircle in the low-frequency region. The corrosion resistance is distinguished by the larger dimension of the capacitive loop.

**Fig. 5** XRD correspond to the EIS reaction products after 2 W immersion

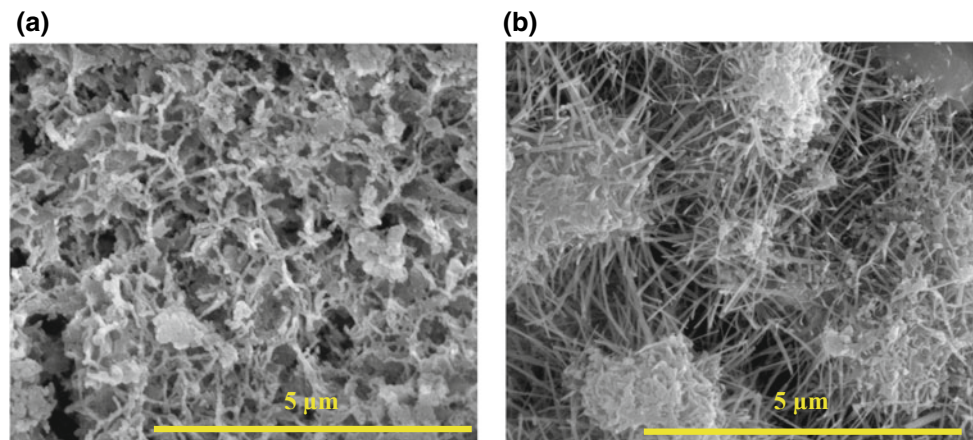


It can be seen from Figs. 1a, 2a, and 3a, that the composition with 7ES has the lowest polarization resistance of  $225 \Omega \text{ cm}^2$  after 2 weeks immersion. Mg-2.5Zn alloy has the maximum polarization resistance of  $590 \Omega \text{ cm}^2$  for the same duration. These changes were attributed to mass transportation, charge transfer reaction, and pitting corrosion during the in vitro degradation process.

Figure 4 illustrates the Tafel curves of the Mg alloys in SBF solution. It can be noticed that Mg-Zn alloy has the lowest corrosion current density of  $29 \mu\text{A cm}^{-2}$  in comparison with 33 and  $37 \mu\text{A cm}^{-2}$  of Mg-2.5Zn-3ES and Mg-2.5Zn-7ES alloys, respectively. These results are matching with the EIS measurements for the 1st-day immersion of Mg-2.5Zn alloys.

To understand the morphology of the corroded sample surfaces, SEM analyses were employed. As depicted in Figs. 1b, 2b, and 3b clear morphological changes were observed due to the immersion in SBF for 2 W. The reaction products were loose and distributed on the surface of the corroded samples. There were various cracks developed on the degraded sample surfaces and can be attributed to the sample shrinkage during drying. The XRD patterns in Fig. 5 elucidate the reaction products after immersion of 336 h, which is in good agreement with earlier findings [10, 21].

**Fig. 6** Growth of needle like apatite due to addition of ES particles **a** 3ES, **b** 7ES



Growth of apatite [22] is observed in Fig. 6a, b due to the interaction of ES particle with SBF during the two weeks of immersion.

## Conclusion

The work demonstrated the in vitro degradation behaviour of Mg–2.5Zn alloy and Mg–2.5Zn–xES composite. The in vitro degradation was carried in simulated body fluid using electrochemical impedance spectroscopy. The EIS and Tafel plots indicated Mg–2.5Zn alloy has good corrosion resistance. 3ES eco-composite is relatively lower in the corrosion resistance than that of Mg–2.5Zn alloy after 2 weeks of immersion. The pitting corrosion is the dominant corrosion mechanism in all the tested samples. Apatite growth is observed on the eco-composite specimens after two weeks of immersion electrochemical analysis.

## References

- Abbassi F, Srinivasan M, Loganathan C, Narayanasamy R, Gupta M (2016) Experimental and numerical analyses of magnesium alloy hot workability. *J Mag All* 4(4), 295–301
- Niinomi M, Nakai M, Hieda J (2012) Development of new metallic alloys for biomedical applications. *Acta Bio* 8(11), 3888–3903
- Gupta M (2018) A snapshot of remarkable potential of mg-based materials as implants. *Mat Sci Eng Int J* 2(1), 30–33
- Jafari S, Raman RS (2017) In-vitro biodegradation and corrosion-assisted cracking of a coated magnesium alloy in modified-simulated body fluid. *Mater Sci Eng C* 78, 278–287
- Johnston S, Shi Z, Venezuela J, Wen C, Dargusch MS, Atrons A (2019) Investigating Mg biocorrosion in vitro: lessons learned and recommendations. *JOM*, 71(4), 1406–1413
- Parande G, Manakari V, Meenashisundaram GK, Gupta M (2016) Enhancing the hardness/compression/damping response of magnesium by reinforcing with biocompatible silica nanoparticulates. *Int J Mater Res* 107(12), 1091–1099
- Jingyuan Y, Jianzhong W, Qiang L, Jian S, Jianming C, Xudong S (2016) Effect of Zn on Microstructures and Properties of Mg-Zn Alloys Prepared by Powder Metallurgy Method. *Rar Met Mater Engi* 45(11), 2757–2762
- Li H, Zhen Y, Qin L (2014) Progress of biodegradable metals. *Prog Natur Sci Mat Int* 24(5), 414–422
- O'Neill E, Awale G, Daneshmandi L, Umerah O, Lo KWH (2018) The roles of ions on bone regeneration. *Dru disc tod* 23(4), 879–890
- Kattimani V, Lingamaneni KP, Yalamanchili S, Mupparapu M (2019) Use of eggshell-derived nano-hydroxyapatite as novel bone graft substitute—A randomized controlled clinical study. *J biomat appl* 34(4), 597–614
- Lee SW, Kim SG, Balázs C, Chae WS, Lee HO (2012) Comparative study of hydroxyapatite from eggshells and synthetic hydroxyapatite for bone regeneration. *Or sur or med or path or rad* 113(3), 348–355
- Kumar GS, Girija EK (2013) Flower-like hydroxyapatite nanostructure obtained from eggshell: A candidate for biomedical applications. *Cer Int* 39(7), 8293–8299
- Parande G, Manakari V, Koppa SDS, Gupta M (2018) Utilizing Low-Cost Eggshell Particles to Enhance the Mechanical Response of Mg–2.5 Zn Magnesium Alloy Matrix. *Adv Eng Mat*, 20(5), 1700919
- Lu H, Wang X, Zhang T, Cheng Z, Fang Q (2009) Design, fabrication, and properties of high damping metal matrix composites—a review. *Mater* 2(3), 958–977
- Chen Y, Shim VPW, Gupta M (2014) Dynamic Tensile Response of Magnesium Nanocomposites. *Appl Mech Mat* 566, 56–60
- Srinivasan M, Loganathan C, Narayanasamy R, Senthilkumar V, Nguyen QB, Gupta M (2013) Study on hot deformation behavior and microstructure evolution of cast-extruded AZ31B magnesium alloy and nanocomposite using processing map. *Mat Des* 47, 449–455
- Meenashisundaram G, Nai M, Gupta M (2015). Effects of primary processing techniques and significance of hall-petch strengthening on the mechanical response of magnesium matrix composites containing TiO<sub>2</sub> nanoparticulates. *Nanomater* 5(3), 1256–1283
- Nguyen QB, Gupta M (2010) Enhancing compressive response of AZ31B using nano-Al<sub>2</sub>O<sub>3</sub> and copper additions. *J All Comp* 490 (1–2), 382–387
- El-Haddad MA, Radwan AB, Sliem MH, Hassan WM, Abdullah AM (2019) Highly efficient eco-friendly corrosion inhibitor for mild steel in 5 M HCl at elevated temperatures: experimental & molecular dynamics study. *Sci rep* 9(1), 3695

20. Kokubo T, Takadama H (2006) How useful is SBF in predicting in vivo bone bioactivity? *Biomater* 27(15), 2907–2915
21. Sunil BR, Kumar AA, Kumar TS, Chakkingal U (2013) Role of biomineralization on the degradation of fine grained AZ31 magnesium alloy processed by groove pressing. *Mat Science Eng C* 33(3), 1607–1615
22. Harandi SE, Mirshahi M, Koleini S, Idris MH, Jafari H, Kadir MR (2013) Effect of calcium content on the microstructure, hardness and in-vitro corrosion behavior of biodegradable Mg-Ca binary alloy. *Mat Res* 16(1), 11–18